Approximate P-wave reflection coefficient in weakly-to-moderately anisotropic media of arbitrary tilt

Véronique Farra [1] and Ivan Pšenčík [2,3]

[1]Université de Paris, Institut de Physique du Globe de Paris, UMR 7154 CNRS, Paris, France. E-mail: farra@ipgp.fr
[2]Institute of Geophysics, Acad. Sci. of CR, Boční II, 141 31 Praha 4, Czech Republic. E-mail: ip@ig.cas.cz
[3]Charles University, Faculty of Mathematics and Physics, Department of Geophysics, Ke Karlovu 3, 121 16 Praha 2, Czech Republic

Summary

There is an evident need for simple and transparent approximate formulae for reflection/transmission coefficients, which could find applications in the amplitude-versus-offset (AVO) or amplitude-versus-azimuth (AVA) studies. It is desirable that such formulae are applicable to a broad type of media, and parameterized in a unique way utilizable in other related studies. We offer such an approximate formula for the P-wave reflection coefficient. It is based on the weak-contrast and weak-anisotropy approximations. The coefficient is applicable to any type of weak-to-moderate anisotropy. It is specified in terms of weak-anisotropy (WA) parameters, which represent an alternative to the commonly used elements of the stiffness matrix. They represent a unique set of parameters capable to describe any type of anisotropy. They can also be used for the specification of other related concepts as the reflection moveout or the geometrical spreading. Presented tests illustrate high accuracy and flexibility of the formula.

Introduction

P-wave reflection coefficients play an important role in the amplitude-versus-offset (AVO) or amplitude-versus-azimuth (AVA) studies. In isotropic media or transversely isotropic (TI) media with vertical axis of symmetry (VTI media), explicit, but rather complicated formulae for P-wave reflection coefficients exist (Červený, 2001; Daley and Hron, 1977). For anisotropic media of lower symmetry, P-wave reflection coefficient and other reflection and transmission coefficients are usually calculated by solving a system of linear algebraic equations (Fedorov, 1968; Gajewski and Pšenčík, 1987). In all mentioned cases, it is difficult to seek how individual parameters specifying the anisotropic medium affect the coefficients, and through them, AVO or AVA data. For this reason, various approximations of reflection and transmission coefficients are sought. First natural approximation is the assumption of a weak contrast of velocities across an interface,

Seismic Waves in Complex 3–D Structures, **30** (2020), 47–61 (ISSN 2336–3827, online at http://sw3d.cz)

see, for example, Ursin and Haugen (1996), Rüger (1997), Golikov and Stovas (2010), Jin and Stovas (2020a). Another frequent approximation is the weak-anisotropy approximation, see, for example, Rüger (1997), Zillmer et al. (1997), Vavryčuk and Pšenčík (1998), Pšenčík and Martins (2001), Ivanov and Stovas (2017).

There is a variety of publications, in which their authors treat the above-described problem of the reflection or transmission differently. Klimeš (2003), for example, presents reflection/transmission formulae for weak-contrast interface separating media of general, arbitrarily strong anisotropy. Most of the considered coefficients are displacement reflection/transmission coefficients, some authors use, however, coefficients normalized with respect to the vertical energy flux (Zillmer et al., 1997; Jin and Stovas, 2020a, b). In many studies, the authors use Thomsen (1986) parameters or their various generalizations varying from one anisotropy symmetry to another.

In this study, we use the weak-contrast and weak-anisotropy approximations and present an approximate formula for P-wave displacement reflection coefficient applicable to weak-contrast interfaces surrounded by weakly-to-moderate anisotropic media of arbitrary anisotropy symmetry and orientation. For the parameterization of the medium, we use weak-anisotropy (WA) parameters, which represent a generalization of VTI parameters introduced by Thomsen (1986). WA parameters are an alternative of elements of the stiffness matrix, commonly used for the description of anisotropy (Fedorov, 1968; Červený, 2001). They can be easily transformed from one Cartesian coordinate system to another, which makes them a very useful tool for studying wave propagation in arbitrary anisotropic media. They are especially efficient when they are used within the weak-anisotropy approximations of wave propagation in anisotropic media.

In the following, we consider three Cartesian coordinate systems, *global*, *profile* and *crystal* coordinate systems. The x_3 axis of the global coordinate system is vertical, positive downwards. The axes x_1 and x_2 are situated in the horizontal plane so that the coordinate system is right-handed. The profile coordinate system x'_i shares its x'_3 axis with the x_3 axis of the global coordinate system, its horizontal axes x'_1 and x'_2 may be rotated with respect to the horizontal axes of the global coordinate system. The coordinate planes or axes of the crystal coordinate system coincide with the symmetry elements of the studied anisotropy medium. In the TI case, the third coordinate axis of the crystal coordinate system is identical with the axis of symmetry of the TI medium. In the orthorhombic case, the coordinate axes are parallel with the intersections of symmetry planes. The crystal coordinate system may be rotated with respect to the profile or global coordinate system. This rotation can be specified either by three unit vectors specifying coordinate lines of the crystal coordinate system or by three Euler angles φ, θ and ν, see Appendix A for more details.

Approximate P-wave reflection coefficient used in this study is expressed in terms of weak-anisotropy (WA) parameters, see, e.g., Farra et al. (2016). WA parameters may be related to the global coordinate system, and then we call them global WA parameters, or to profile coordinate system, and then we call them profile WA parameters. WA parameters in the crystal coordinate system are usually called after the symmetry, which they specify, e.g., TI WA or OR WA parameters meaning WA parameters specifying transverse isotropy or orthorhombic symmetry, respectively.

The structure of the paper is following. In the following section, we present the approximate formula for the P-wave reflection coefficient. It depends on contrasts of four profile WA parameters. In the section, which follows, we test the accuracy of the formula on two models of different anisotropy symmetry and anisotropy strength. The main part of the paper ends with a short Conclusion. The paper is supplemented by two Appendices. In Appendix A, WA parameters are introduced, and it is shown how the four profile WA parameters, on which the reflection coefficient depends, can be expressed in terms of tilted TI or orthorhombic symmetry. Appendix B contains specifications of anisotropy parameters of models used in synthetic tests.

Theoretical background

The present study is based on the approximate equation for the P-wave reflection coefficient given by Pšenčík and Martins (2001), who transformed P-wave reflection coefficient expressed in terms of elastic parameters $A_{\alpha\beta}$ into the coefficient expressed in terms of WA parameters. We specify equation (7) of Pšenčík and Martins (2001), which is expressed in terms of angles of incidence φ and θ, for $\varphi = 0°$. The angles of incidence, which we denote here φ_i and θ_i, in order to distinguish them from other angles, specify the direction $\mathbf{n}$ of the P-wave slowness vector associated with the coefficient of reflection. The vector $\mathbf{n}$ is situated in the vertical plane (x_1', x_3') of the profile coordinate system:

$$\mathbf{n} \equiv (\cos\varphi_i \sin\theta_i \quad \sin\varphi_i \sin\theta_i \quad \cos\theta_i) \ . \tag{1}$$

Note that the angle φ_i is the angle, which horizontal axes of the profile coordinate system make with horizontal axes of the global coordinate system.

Equation (7) of Pšenčík and Martins (2001) specified for $\varphi_i = 0°$ reads:

$$R_{PP}(\theta_i) = R_{PP}^{iso}(\theta_i) + \frac{1}{2}\Delta\epsilon_z + \frac{1}{2}(\Delta\delta_y - 8\frac{\bar{\beta}^2}{\bar{\alpha}^2}\Delta\gamma_y - \Delta\epsilon_z)\sin^2\theta_i + \frac{1}{2}\Delta\epsilon_x \sin^2\theta_i \tan^2\theta_i \ . \tag{2}$$

The symbol R_{PP}^{iso} denotes the P-wave reflection coefficient in the reference model consisting of two isotropic half-spaces:

$$R_{PP}^{iso}(\theta_i) = \frac{1}{2}\frac{\Delta Z}{\bar{Z}} + \frac{1}{2}[\frac{\Delta\alpha}{\bar{\alpha}} - 4\frac{\bar{\beta}^2}{\bar{\alpha}^2}\frac{\Delta G}{\bar{G}}]\sin^2\theta_i + \frac{1}{2}\frac{\Delta\alpha}{\bar{\alpha}}\sin^2\theta_i \tan^2\theta_i \ . \tag{3}$$

Here

$$Z = \rho\alpha, \quad G = \rho\beta^2 \ . \tag{4}$$

The symbols Δ are used to denote the contrasts of quantities between the lower half-space (quantities with subscript 2) and the upper half-space (quantities with subscript 1), e.g., $\Delta\alpha = \alpha_2 - \alpha_1$. Bar over a symbol denotes an average, e.g. $\bar{\alpha} = 1/2(\alpha_1 + \alpha_2)$. The symbols α and β denote P- and S-wave velocities of the reference isotropic half-spaces. As mentioned above, the symbol θ_i denotes one of the incidence angles, the other angle, φ_i, is chosen $\varphi_i = 0°$.

We can see that the P-wave reflection coefficient depends on contrasts of four profile WA parameters, ϵ_x, ϵ_z, δ_y and γ_y specified in the profile coordinate system. The reference velocities α and β used in equation (3) are also used as the reference velocities defining the WA parameters, see equation (A-1). As shown in Farra and Pšenčík (2017) or Pšenčík and Farra (2017), the above four profile WA parameters can be expressed in terms of WA parameters of an orthorhombic or TI medium specified in the crystal coordinate system. In Appendix A, we provide the transformation relations between the above WA parameters ϵ_x, ϵ_z, δ_y and γ_y and WA parameters in media of orthorhombic or TI symmetry.

The above-described specification of the P-wave reflection coefficient (2) has a series of advantages. First, it can be applied to weak-to-moderate anisotropy of any symmetry. Second, the used WA parameters can be used for the description of any anisotropic symmetry. There is no need to change the parameterization when shifting from one symmetry to another. Third, the use of WA parameters allows to vary the choice of the reference velocities. Since we are interested in the use of reflection coefficients for prevailingly small angles of incidence (directions close to vertical), it is preferable to use velocities close or equal to vertical velocities as the reference velocities. The formula (2) is simple and transparent. Description of additional advantages can be found in Pšenčík and Martins (2001).

Tests of accuracy

We test the accuracy of equation (2) on two models. One with relatively weak anisotropy and weak velocity contrast of the reference isotropic medium, the other with much stronger anisotropy and stronger velocity contrast.

The first model, taken from the study of Ivanov and Stovas (2017), which we call ISO/TTI, consists of an isotropic upper half-space and bottom half-space of transverse isotropy with tilted axis of symmetry (TTI). The density is the same in both half-spaces and equals $\rho_1 = \rho_2 = 2.7$ g/cm^3. P- and S-wave velocities in the isotropic half-space are α_1=2.37 and β_1 =1.36 km/s. The bottom half-space is formed by the TTI symmetry whose matrix of the density-normalized elastic moduli in the Voigt notation is shown in equation (B-1). The matrix was reconstructed from the values of Thomsen's (1986) parameters used by Ivanov and Stovas (2017). Corresponding WA parameters in the crystal coordinate system, with the reference P- and S-wave velocities $\alpha_2 = 2.37$ and β_2 =1.36 km/s are $\epsilon_x^{TI} = 0.05$, $\epsilon_z^{TI} = 0.$, $\delta_y^{TI} = 0.02$, $\gamma_y^{TI} = 0.$ and $\gamma_z^{TI} = 0.1$. WA parameters ϵ_z^{TI} and γ_y^{TI} are zero because of the choice of the reference velocities as velocities along the axis of symmetry. The strength of anisotropy is relatively low, around 5%.

The second model, taken from Neves and de Hoop (2000), which we call here VTI/TOR, is the model consisting of the VTI upper half-space underlaid by the half-space of orthorhombic symmetry with tilted planes (axes) of symmetry (TOR). The densities in the upper and bottom half-spaces are $\rho_1 = 2.5$ and $\rho_2 = 2.2$ g/cm^3, respectively. The matrices of the density-normalized elastic moduli in the Voigt notation in the crystal coordinate systems are shown in equations (B-2) and (B-3). The matrix (B-3) is rotated by the matrix given in equation (A-3) to make the bottom half-space of TOR symmetry. The rotation from the global coordinate system is specified by the Euler angles $\varphi = 0°$, $\theta = 30°$ and $\nu = 0°$. WA parameters in the crystal coordinate system, with reference P- and S-wave velocities $\alpha_1 = 2.07$ and β_1 =1.11 km/s, corresponding to the matrix (B-2) are $\epsilon_x^{TI} = 0.31$, $\epsilon_z^{TI} = 0.$, $\delta_y^{TI} = 0.21$, $\gamma_y^{TI} = 0.$ and $\gamma_z^{TI} = 0.17$. WA parameters in the crystal coordinate system, with reference P- and S-wave velocities $\alpha_2 = 2.85$ and β_2 =1.48 km/s, corresponding to the matrix (B-3), are $\epsilon_x^{OR} = 0.26$, $\epsilon_y^{OR} = 0.33$, $\epsilon_z^{OR} = 0.$, $\delta_x^{OR} = 0.08$, $\delta_y^{OR} = -0.09$, $\delta_z^{OR} = 0.33$, $\gamma_x^{OR} = 0.12$, $\gamma_y^{OR} = 0.$ and $\gamma_z^{OR} = 0.18$. WA parameters ϵ_z^{TI}

and γ_y^{TI} are zero because of the choice of the reference velocities as velocities along the axis of symmetry of the TI medium. WA parameters ϵ_z^{OR} and γ_y^{OR} are zero because of the choice of the reference velocities as $\alpha^2 = A_{33}^{OR}$ and $\beta^2 = A_{55}^{OR}$. The strength of anisotropy is in both half-spaces relatively large, around 24%.

The plots in Figures 1 and 2 show reflection coefficient for $\varphi_i = 0°$, as a function of the angle of incidence θ_i. Four values of the Euler angle φ specifying the rotation of the axis of symmetry with respect to the global coordinate system in the bottom half-space, $\varphi = 0°$, 30°, 60° and 90° are considered. Exact coefficients are shown by bold curves, approximate coefficients calculated from equation (2) by thin curves of the same colour. Black colour corresponds to $\theta = 0°$, i.e., to the VTI case, red to $\theta = 30°$, blue to $\theta = 60°$ and green to $\theta = 90°$, i.e., to HTI case. In the plots a) and c), the reference velocities of the TTI medium in the bottom half-space are chosen as the velocities along the axis of symmetry, and in the plots b) and d) as $\alpha^2 = A_{33}$ and $\beta^2 = A_{55}$, where A_{33} and A_{55} are elements of the matrix (B-1) after the above described rotation. The plots a) and c) in Figures 1 and 2 correspond to Figure 3 of Ivanov and Stovas (2017). Although equation (2) should correspond to equation (17) of Ivanov and Stovas (2017), WA parameter δ does not differ much from δ of Thomsen (1986) used by Ivanov and Stovas (2017), and the reference velocities are chosen the same, the results based on equation (2) yield surprisingly better fit, especially for larger angles of incidence θ_i. The best fit of approximate and exact results in the plots a) and c) can be observed for zero tilt (VTI case - black curve) and also for tilt of 30° (red curve). Visible differences can be observed for larger tilts (green and blue curves). They are caused by the more significant difference between actual vertical velocities and the used reference velocities. These differences disappear in the plots b) and d) of Figures 1 and 2. As mentioned above, in these plots, the reference velocities are chosen close to vertical velocities. Due to this choice, one can observe better fit of approximate and exact reflection coefficients in plots b) and d) in both figures. Comparison of the plots a) and c) with the plots b) and d) illustrates the advantage of the use of WA parameters, which allow variation of reference velocities. In Thomsen (1986) style parameters, the reference velocities are implicitly taken as velocities along the axis of symmetry. It is necessary to emphasize again that the good performance of the approximate equation (2) is also caused by relatively weak anisotropy.

In Figures 3 and 4, we show results for the model VTI/TOR, which is characterized by considerably stronger anisotropy than the previous ISO/TTI model. Display of results in Figures 3 and 4 is different from that in Figures 1 and 2. In Figures 3 and 4, coefficients or their differences are shown for azimuths φ_i running from 0° to 90° and angles of incidence θ_i running from 10° to 30°. The plot a) in Figure 3 shows the variation of the exact P-wave reflection coefficient. The plot b) in Figure 3 and the plots a) and b) in Figure 4 show differences of the approximate coefficient (2) from the exact coefficient. Reference velocities in the upper layer are velocities along the axis of symmetry, i.e., vertical. The plots differ by different specification of reference velocities in the bottom layer. In the bottom half-space of the model in Figure 3b, the reference velocities are chosen in the following way: $\alpha^2 = A_{33}$ and $\beta^2 = A_{55}$. Here A_{33} and A_{55} are the elements of the matrix (B-3) after the above described rotation. Despite relatively strong anisotropy, the differences of values of the approximate formula (2) and exact results are rather small. In the left part of the plot, the approximate coefficient is slightly greater than the exact one. The difference is less than 0.002. In the right part of the plot, the approximate coefficient

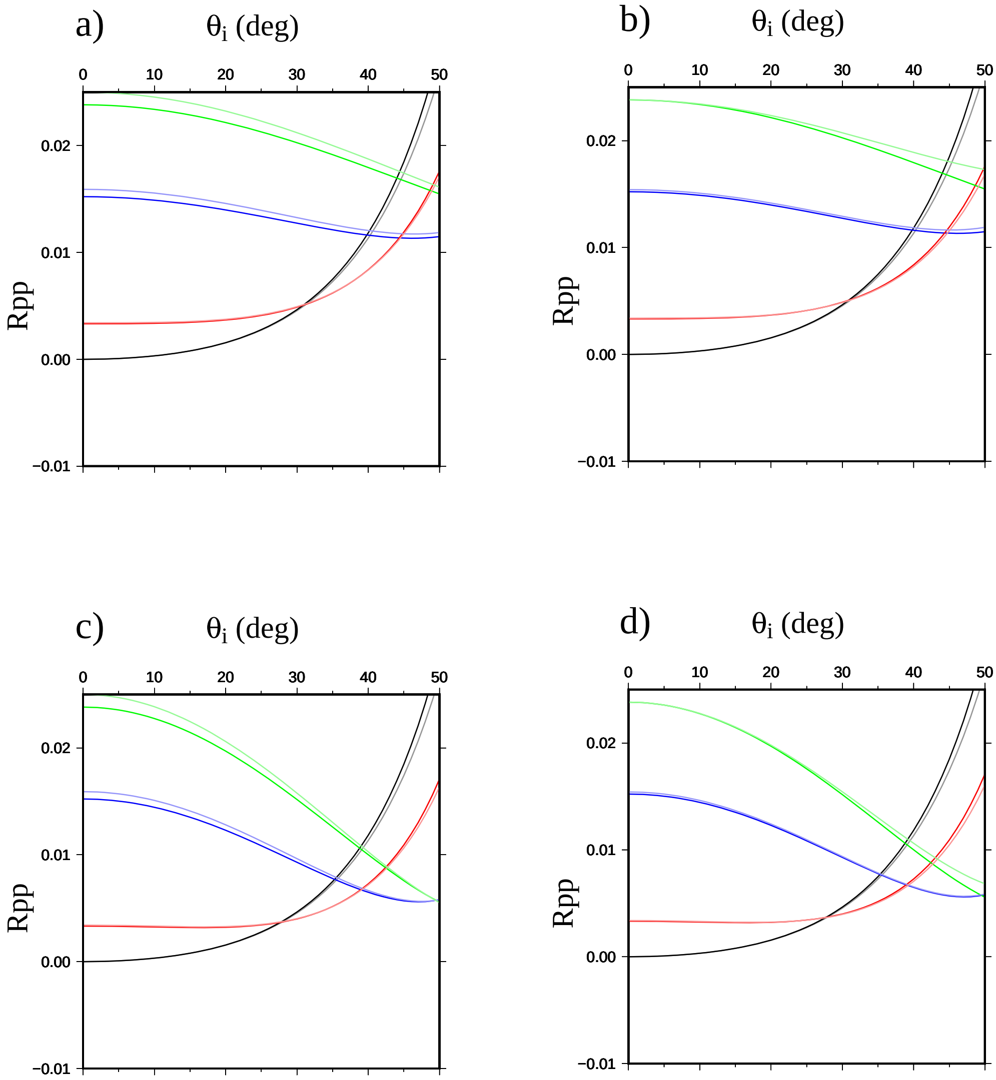

Figure 1: Comparison of exact (bold) and approximate (thin) P-wave reflection coefficients at the reflector separating upper isotropic and bottom TTI half-spaces. The model corresponds to the model used by Ivanov and Stovas (2017) in their Figure 3. Isotropic half-space parameters are $\alpha_1 = 2.37$ km/s, $\beta_1 = 1.36$ km/s and $\rho = 2.7$ g/cm^3. The density is the same in the bottom half-space. Velocities α_2 and β_2 are specified as velocities along the axis of symmetry in the plots a) and c), and as $\alpha^2 = A_{33}$ and $\beta^2 = A_{55}$ in the plots b) and d). A_{33} and A_{55} are elements of the correspondingly rotated matrix (B-1). WA parameters in the crystal coordinate system are given in the text. The axis of symmetry of the TTI half-space is specified by the azimuth φ and tilt θ. Results for $\varphi = 0°$ are shown in the plots a) and b), for $\varphi = 30°$ in c) and d). Black colour corresponds to $\theta = 0°$ (VTI), red to $\theta = 30°$, blue to $\theta = 60°$ and green to $\theta = 90°$ (HTI).

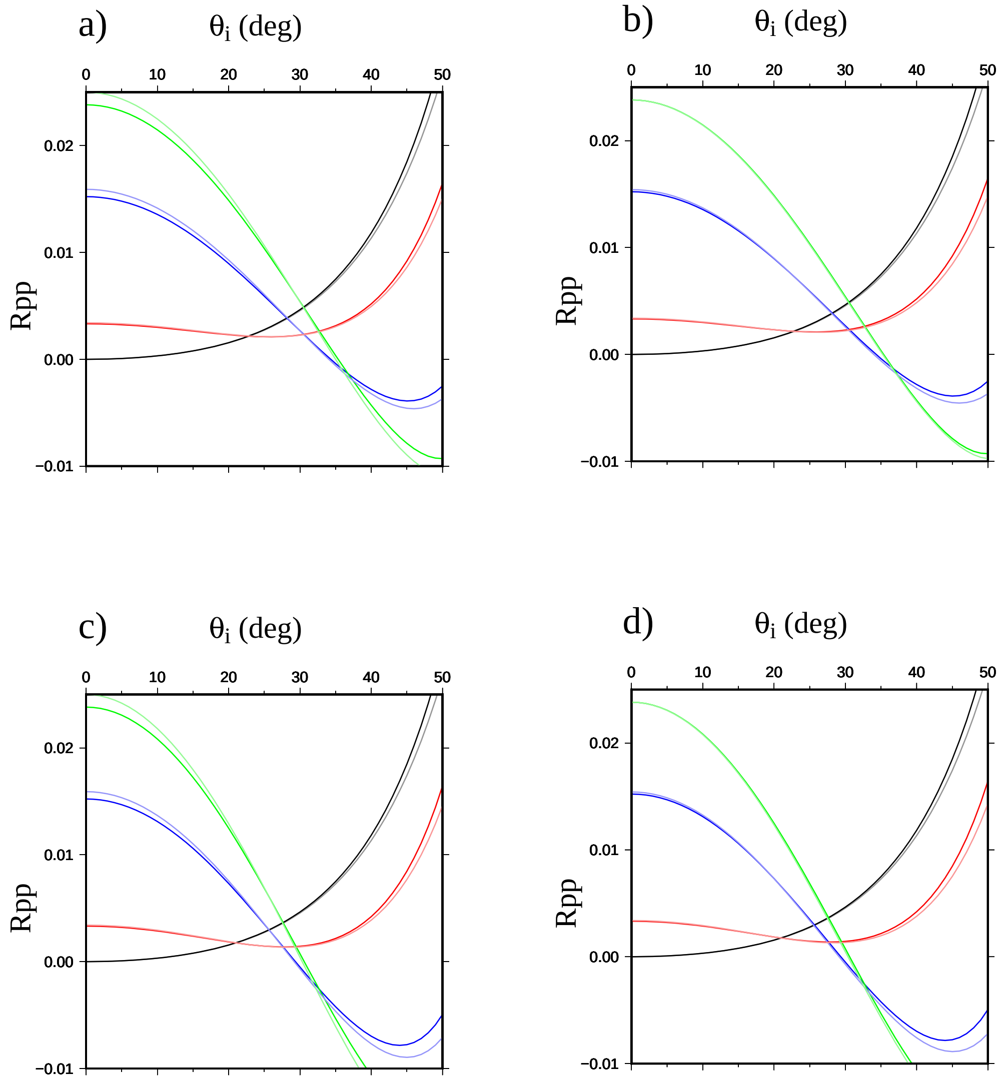

Figure 2: Comparison of exact (bold) and approximate (thin) P-wave reflection coefficients at the reflector separating upper isotropic and bottom TTI half-spaces. The model corresponds to the model used by Ivanov and Stovas (2017) in their Figure 3. Isotropic half-space parameters are $\alpha_1 = 2.37$ km/s, $\beta_1 = 1.36$ km/s and $\rho = 2.7$ g/cm^3. The density is the same in the bottom half-space. Velocities α_2 and β_2 are specified as velocities along the axis of symmetry in the plots a) and c), and as $\alpha^2 = A_{33}$ and $\beta^2 = A_{55}$ in the plots b) and d). A_{33} and A_{55} are elements of the correspondingly rotated matrix (B-1). WA parameters in the crystal coordinate system are given in the text. The axis of symmetry of the TTI half-space is specified by the azimuth φ and tilt θ. Results for $\varphi = 60°$ are shown in the plots a) and b), for $\varphi = 90°$ in c) and d). Black colour corresponds to $\theta = 0°$ (VTI), red to $\theta = 30°$, blue to $\theta = 60°$ and green to $\theta = 90°$ (HTI).

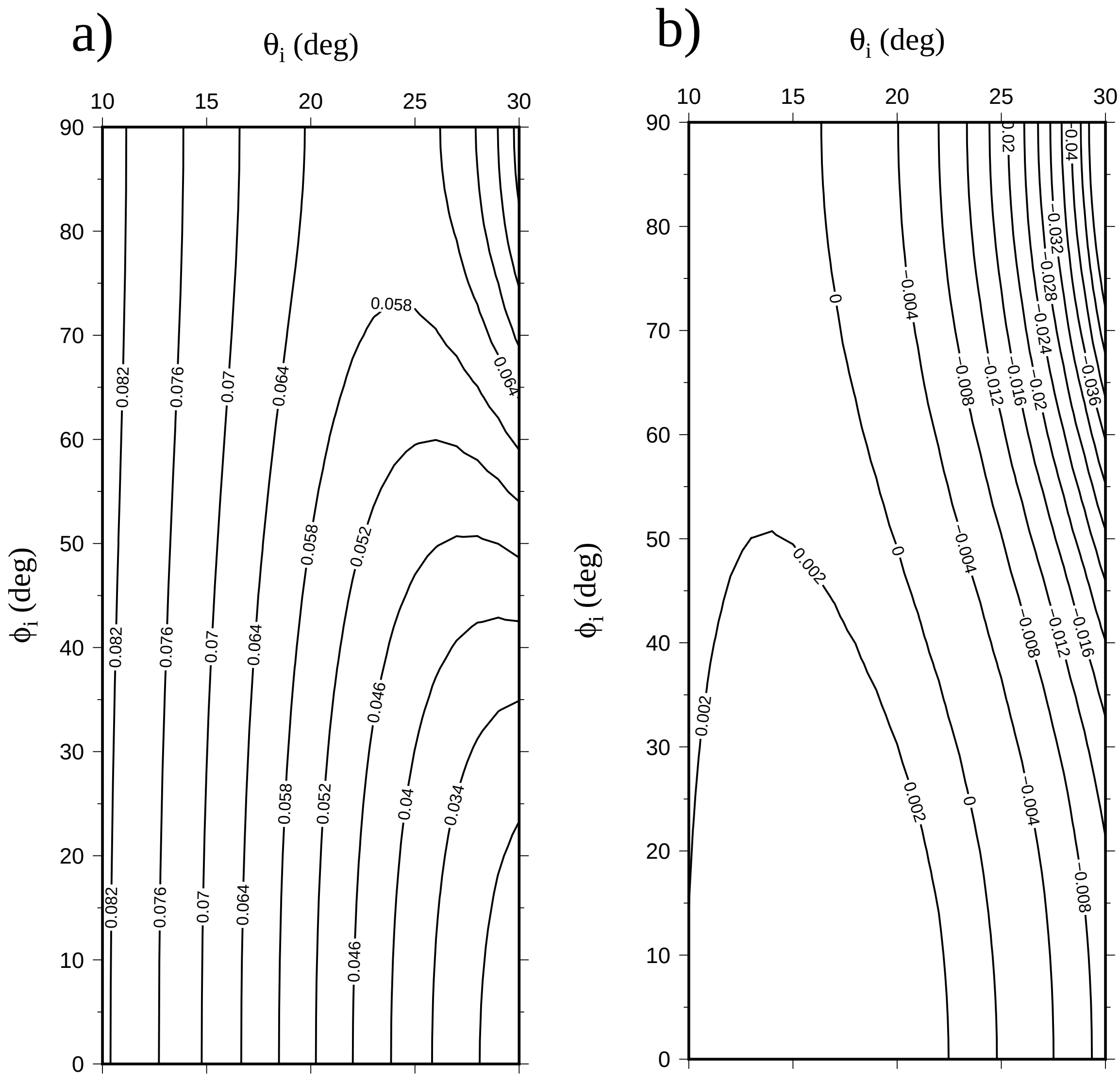

Figure 3: The map of a) exact P-wave reflection coefficient and b) of absolute errors of the approximate coefficient (2) in the VTI/TOR model specified by the matrices of the density-normalized elastic parameters (B-2) and (B-3). The upper half-space is VTI, the lower half-space is TOR specified by the Euler angles $\varphi = 0°$, $\theta = 30°$ and $\nu = 0°$, see the matrix (A-3). Reference P- and S-wave velocities in the upper half-space of the plot b) are taken along the vertical, in the bottom half-space, they are specified as $\alpha^2 = A_{33}$ and $\beta^2 = A_{55}$, where A_{33} and A_{55} are elements of the rotated matrix (B-3). The angles φ_i and θ_i are the angles of incidence.

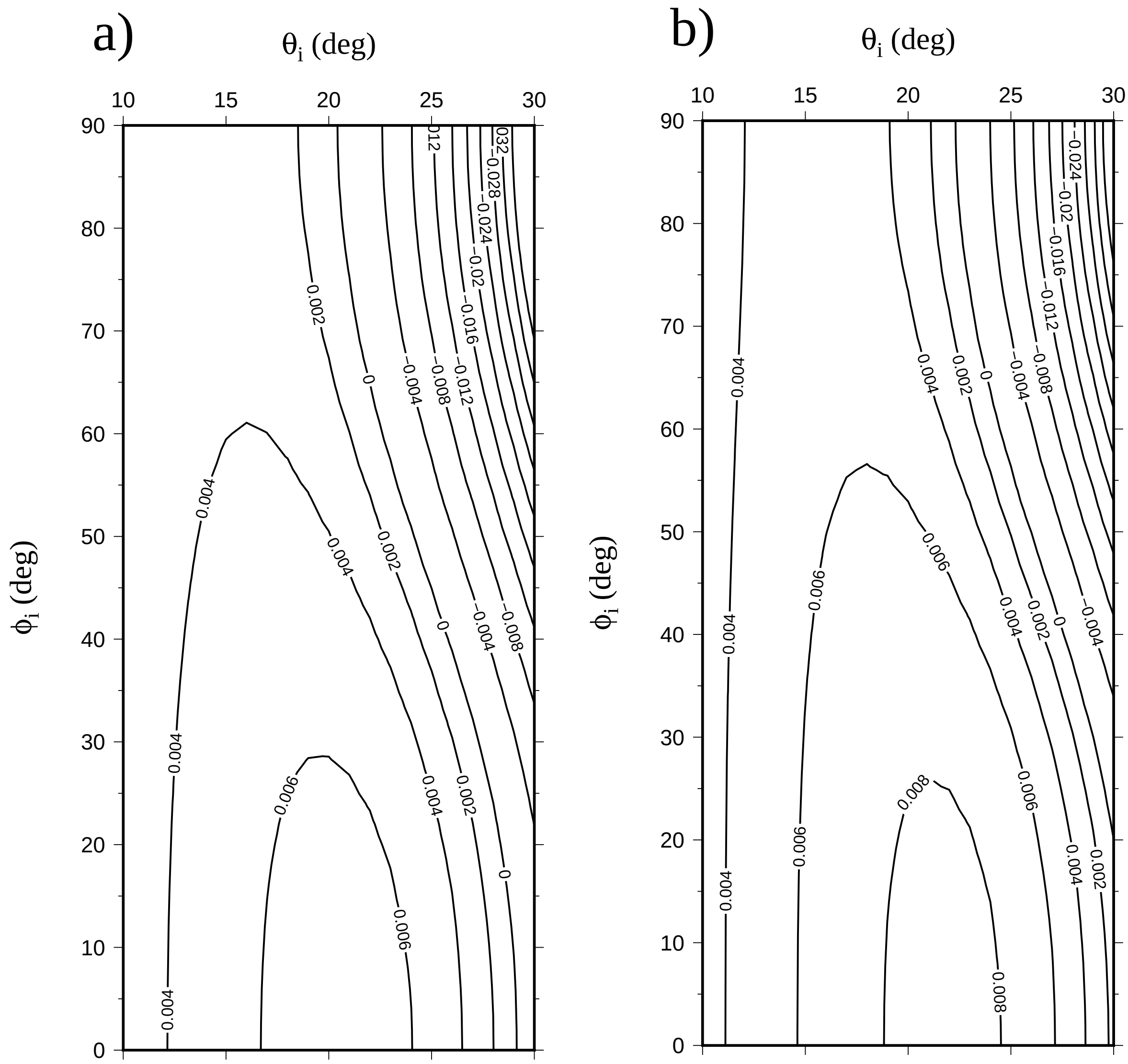

Figure 4: The map of absolute errors of the approximate coefficient (2) in the VTI/TOR model specified by the matrices of the density-normalized elastic parameters (B-2) and (B-3). The upper half-space is VTI, the lower half-space is TOR specified by the Euler angles $\varphi = 0°$, $\theta = 30°$ and $\nu = 0°$, see the matrix (A-3). Reference P- and S-wave velocities in the upper and lower half-spaces are taken as velocities along the axis of symmetry. In the TOR half-space $\alpha^2 = A^{OR}_{33}$ and a) $\beta^2 = A^{OR}_{44}$ and b) $\beta^2 = A^{OR}_{55}$. The angles φ_i and θ_i are the angles of incidence.

is smaller than the exact one. For great φ_i, up-to approximately $\theta_i = 22°$ and more, the absolute differences do not exceed 0.008. Then they start to increase significantly. For small φ_i, the region of absolute differences less than 0.008 extends to nearly $\theta_i = 30°$. In Figures 4a and 4b, the reference velocities in the bottom layer are chosen as velocities along the intersection of vertical symmetry planes in the crystal coordinate system. Specifically they are chosen as follows: $\alpha^2 = A_{33}^{OR}$ and $\beta^2 = A_{44}^{OR}$ in Figure 4a and $\alpha^2 = A_{33}^{OR}$ and $\beta^2 = A_{55}^{OR}$ in Figure 4b. Overall behaviour of the approximate coefficients is similar to that in Figure 3b, the approximate coefficient is greater that the exact one in the left part of the plot and smaller in the right part. We can see that the choice of reference velocities leads to the increase of differences with respect to Figure 3b for small values of the angle of incidence θ_i, and to their stronger variation with φ_i. For larger values of θ_i, the differences are, however, smaller than in Figure 3b. From comparison of Figures 4a and 4b, one can see that the choice of the reference S-wave velocity may affect the accuracy of the formula (2).

Conclusion

Approximate formula for the reflection coefficient of unconverted P wave applicable to arbitrary weak-to-moderate anisotropic media is presented and tested. The formula is based on the weak-contrast and weak-anisotropy approximations. It is expressed in terms of weak-anisotropy parameters, which can be used for specification of any type of anisotropy. Their easy transformation (alternative of Bond transformation) from one coordinate system to another allows simple dealing with arbitrarily tilted anisotropies. Another advantage is the freedom of choice of the reference velocity of WA parameters, which allows to choose the reference velocity as close as possible to the actual velocity and, in this way, to make the calculations more accurate. Last, but not least, advantage of the parameterization by WA parameters is that there are approximate formulae for the reflection moveout and the relative geometrical spreading also expressed in terms of WA parameters. This means that WA parameters can be used as a unique tool for the approximate evaluation of all mentioned quantities, and this tool is applicable to arbitrary anisotropy. The only limitation is the weak-anisotropy assumption, which leads to the decrease of accuracy of the approximate formulae with increasing strength of anisotropy. Performed tests show that the accuracy of the formula for the P-wave reflection coefficient is quite high even when anisotropy strength exceeds 20%.

The presented procedure could be used equally well for the specification of the P-wave transmission coefficient. Generalization for S waves and converted waves would be more complicated, but also feasible.

Acknowledgement

We are grateful to the project "Seismic waves in complex 3-D structures" (SW3D) and the Research Project 20-06887S of the Grant Agency of the Czech Republic for support.

Appendix A

WA parameters and their transformations

The complete set of 21 WA parameters is defined as follows:

$$\epsilon_x = \frac{A_{11}-\alpha^2}{2\alpha^2}\ , \quad \epsilon_y = \frac{A_{22}-\alpha^2}{2\alpha^2}\ , \quad \epsilon_z = \frac{A_{33}-\alpha^2}{2\alpha^2}\ ,$$
$$\delta_x = \frac{A_{23}+2A_{44}-\alpha^2}{\alpha^2}\ , \quad \delta_y = \frac{A_{13}+2A_{55}-\alpha^2}{\alpha^2}\ , \quad \delta_z = \frac{A_{12}+2A_{66}-\alpha^2}{\alpha^2}\ ,$$
$$\chi_x = \frac{A_{14}+2A_{56}}{\alpha^2}\ , \quad \chi_y = \frac{A_{25}+2A_{46}}{\alpha^2}\ , \quad \chi_z = \frac{A_{36}+2A_{45}}{\alpha^2}\ ,$$
$$\epsilon_{15} = \frac{A_{15}}{\alpha^2}\ , \quad \epsilon_{16} = \frac{A_{16}}{\alpha^2}\ , \quad \epsilon_{24} = \frac{A_{24}}{\alpha^2}\ , \quad \epsilon_{26} = \frac{A_{26}}{\alpha^2}\ , \quad \epsilon_{34} = \frac{A_{34}}{\alpha^2}\ , \quad \epsilon_{35} = \frac{A_{35}}{\alpha^2}\ ,$$
$$\epsilon_{46} = \frac{A_{46}}{\beta^2}, \quad \epsilon_{56} = \frac{A_{56}}{\beta^2}, \quad \epsilon_{45} = \frac{A_{45}}{\beta^2},$$
$$\gamma_x = \frac{A_{44}-\beta^2}{2\beta^2}, \quad \gamma_y = \frac{A_{55}-\beta^2}{2\beta^2}, \quad \gamma_z = \frac{A_{66}-\beta^2}{2\beta^2}\ . \qquad (A-1)$$

The symbols $A_{\gamma\delta}$, γ, δ=1, 2, ...,6, denote the density normalized elastic moduli in the Voigt notation, α and β denote the reference P- and S-wave velocities in the reference isotropic medium.

Profile WA parameters ϵ_x, ϵ_z, δ_y and γ_y appearing in the approximate expression for the reflection coefficient can be expressed in terms of WA parameters specified in the crystal coordinate system, see Farra and Pšenčík (2017) for orthorhombic media and Pšenčík and Farra (2017) for transversely isotropic media.

Let us specify the axes of the crystal coordinate system in the profile or global coordinate system by three unit, mutually perpendicular, vectors $\mathbf{t}$, $\mathbf{e}$ and $\mathbf{n}$. Then the rotation matrix $\mathbf{R}$ from the crystal to the profile coordinate system can expressed as:

$$\mathbf{R} = \begin{pmatrix} n_1 & e_1 & t_1 \\ n_2 & e_2 & t_2 \\ n_3 & e_3 & t_3 \end{pmatrix}\ . \qquad (A-2)$$

The matrix $\mathbf{R}$ can be rewritten using three Euler angles φ, θ and ν. The Euler angles φ and θ can be understood as azimuth and polar angles specifying the orientation of originally vertical axis of symmetry (intersection of two vertical planes of symmetry). The angle ν then represents a rotation around the new position of this axis. The matrix $\mathbf{R}$ can be then also expressed as:

$$\mathbf{R} = \begin{pmatrix} \cos\varphi\cos\theta\cos\nu - \sin\varphi\sin\nu & -\cos\varphi\cos\theta\sin\nu - \sin\varphi\cos\nu & \cos\varphi\sin\theta \\ \sin\varphi\cos\theta\cos\nu + \cos\varphi\sin\nu & -\sin\varphi\cos\theta\sin\nu + \cos\varphi\cos\nu & \sin\varphi\sin\theta \\ -\sin\theta\cos\nu & \sin\theta\sin\nu & \cos\theta \end{pmatrix}\ . \qquad (A-3)$$

Let us now consider an orthorhombic medium and let us mark its WA parameters in the crystal coordinate system by upper indices OR. In the crystal coordinate system, 9 of

21 WA parameters are non-zero: ϵ_x^{OR}, ϵ_y^{OR}, ϵ_z^{OR}, δ_x^{OR}, δ_y^{OR}, δ_z^{OR}, γ_x^{OR}, γ_y^{OR} and γ_z^{OR}. WA parameters ϵ_x, ϵ_z, δ_y and γ_y appearing in equation (2) relate to the above WA parameters in the crystal coordinate system in the following way:

$$\epsilon_x = \epsilon_x^{OR} n_1^4 + \epsilon_y^{OR} e_1^4 + \epsilon_z^{OR} t_1^4 + \delta_x^{OR} e_1^2 t_1^2 + \delta_y^{OR} n_1^2 t_1^2 + \delta_z^{OR} n_1^2 e_1^2 \ ,$$

$$\epsilon_z = \epsilon_x^{OR} n_3^4 + \epsilon_y^{OR} e_3^4 + \epsilon_z^{OR} t_3^4 + \delta_x^{OR} e_3^2 t_3^2 + \delta_y^{OR} n_3^2 t_3^2 + \delta_z^{OR} n_3^2 e_3^2 \ ,$$

$$\delta_y = 6\epsilon_x^{OR} n_1^2 n_3^2 + 6\epsilon_y^{OR} e_1^2 e_3^2 + 6\epsilon_z^{OR} t_1^2 t_3^2$$

$$+\delta_x^{OR}[(e_1t_3+e_3t_1)^2+2e_1e_3t_1t_3]+\delta_y^{OR}[(t_1n_3+t_3n_1)^2+2t_1t_3n_1n_3]+\delta_z^{OR}[(n_1e_3+n_3e_1)^2+2n_1n_3e_1e_3] \ ,$$

$$\gamma_y = \frac{\alpha^2}{\beta^2}[\epsilon_x^{OR} n_1^2 n_3^2 + \epsilon_y^{OR} e_1^2 e_3^2 + \epsilon_z^{OR} t_1^2 t_3^2$$

$$+\delta_x^{OR} e_1 e_3 t_1 t_3 + \delta_y^{OR} t_1 t_3 n_1 n_3 + \delta_z^{OR} n_1 n_3 e_1 e_3] + \gamma_x^{OR} n_2^2 + \gamma_y^{OR} e_2^2 + \gamma_z^{OR} t_2^2 \ . \qquad (A-4)$$

Let us now consider a TI medium and let us mark its WA parameters in the crystal coordinate system by upper indices TI. In the crystal coordinate system, there are again 9 of 21 WA parameters nonzero, only 5 of them being independent: ϵ_x^{TI}, ϵ_z^{TI}, δ_y^{TI}, γ_y^{TI} and γ_z^{TI}.

The relations between WA parameters ϵ_x, ϵ_z, δ_y and γ_y appearing in equation (2) and the above WA parameters in the crystal coordinate system follow from equations (A-4). If we take the vector $\mathbf{t}$ as a vector parallel to the axis of symmetry, then the vectors $\mathbf{e}$ and $\mathbf{n}$ can be specified as:

$$\mathbf{e} \equiv D^{-1}(t_1t_3, t_2t_3, -D^2), \quad \mathbf{n} \equiv D^{-1}(-t_2, t_1, 0) \ , \qquad (A-5)$$

where

$$D = (t_1^2 + t_2^2)^{1/2}, \quad t_1^2 + t_2^2 + t_3^2 = 1 \ . \qquad (A-6)$$

Equations (A-4) then yield:

$$\epsilon_x = \epsilon_x^{TI}(t_2^2 + t_3^2)^2 + \epsilon_z^{TI} t_1^4 + \delta_y^{TI} t_1^2 (t_2^2 + t_3^2) \ ,$$

$$\epsilon_z = \epsilon_x^{TI}(t_1^2 + t_2^2)^2 + \epsilon_z^{TI} t_3^4 + \delta_y^{TI} t_3^2 (t_1^2 + t_2^2) \ ,$$

$$\delta_y = 2\epsilon_x^{TI}(3t_1^2 t_3^2 + t_2^2) + 6\epsilon_z^{TI} t_1^2 t_3^2 + \delta_y^{TI}(t_1^2 + t_3^2 - 6t_1^2 t_3^2) \ ,$$

$$\gamma_y = \frac{\alpha^2}{\beta^2} t_1^2 t_3^2 (\epsilon_x^{TI} + \epsilon_z^{TI} - \delta_y^{TI}) + \gamma_y^{TI}(1 - t_2^2) + \gamma_z^{TI} t_2^2 \ . \qquad (A-7)$$

The transformation equations (A-4) and (A-7) represent the Bond transformation (Bond, 1943; Chapman, 2004) expressed in terms of WA parameters.

Appendix B

Matrices of the density-normalized elastic moduli in the tested models

Matrices of the density-normalized elastic moduli in the Voigt notation are presented in the crystal coordinate system, in which axes and planes of symmetry of anisotropic media coincide with coordinate axes and planes. In the presented tests, if it were necessary, the matrices were rotated as described in the main text.

Matrix of the density-normalized elastic moduli in $(\mathrm{km/s})^2$ in the lower half-space of the ISO/TTI model (Ivanov and Stovas, 2017) reads:

$$\begin{pmatrix} 6.18 & 1.74 & 2.03 & 0 & 0 & 0 \\ & 6.18 & 2.03 & 0 & 0 & 0 \\ & & 5.62 & 0 & 0 & 0 \\ & & & 1.85 & 0 & 0 \\ & & & & 1.85 & 0 \\ & & & & & 2.22 \end{pmatrix} . \qquad (B-1)$$

Matrices of the density-normalized elastic moduli in $(\mathrm{km/s})^2$ in the VTI/TOR model (Neves and de Hoop, 2000) have the form:

$$\begin{pmatrix} 6.94 & 3.64 & 2.70 & 0 & 0 & 0 \\ & 6.94 & 2.70 & 0 & 0 & 0 \\ & & 4.28 & 0 & 0 & 0 \\ & & & 1.23 & 0 & 0 \\ & & & & 1.23 & 0 \\ & & & & & 1.65 \end{pmatrix} \qquad (B-2)$$

and

$$\begin{pmatrix} 12.27 & 4.87 & 3.05 & 0 & 0 & 0 \\ & 13.44 & 3.31 & 0 & 0 & 0 \\ & & 8.10 & 0 & 0 & 0 \\ & & & 2.70 & 0 & 0 \\ & & & & 2.18 & 0 \\ & & & & & 2.97 \end{pmatrix} . \qquad (B-3)$$

The corresponding P-wave WA parameters for both models are given in the text.

References

Bond, W., 1943, The mathematics of the physical properties of crystals: Bell System Technical Journal, 22, 1–72, doi: 10.1002/j.1538-7305.1943.tb01304.x.

Červený, V., 2001, Seismic Ray Theory: Cambridge Univ. Press, Cambridge.

Chapman, C. H., 2004, Fundamentals of seismic wave propagation: Cambridge University Press.

Daley, P. F., and F. Hron, 1977, Reflection and transmission coefficients for transversely isotropic media: Bull. Seismol. Soc. Am., **67**, 661–675.

Farra, V., and I. Pšenčík, 2013, Moveout approximations for P and SV waves in VTI media: Geophysics, **78**, WC81–WC92.

Farra, V., and I. Pšenčík, 2016, Weak-anisotropy approximations of P-wave phase and ray velocities for anisotropy of arbitrary symmetry: Studia Geophysica et Geodaetica, **60**, 403-418.

Farra, V., I. Pšenčík, and P. Jílek, 2016, Weak-anisotropy moveout approximations for P waves in homogeneous layers of monoclinic or higher anisotropy symmetries: Geophysics, **81**, C39–C59.

Farra, V., and I. Pšenčík, 2017, Weak-anisotropy moveout approximations for P waves in homogeneous TOR layers: Geophysics, **82**, WA23–WA32.

Fedorov, F. I., 1968, Theory of elastic waves in crystals: Plenum Press.

Gajewski, D., and I. Pšenčík, 1987, Computation of high-frequency seismic wavefileds in 3-D laterally inhomogeneous anisotropic media: Geophys.J.R.astr.Soc., **91**, 383–411.

Gajewski, D., and I. Pšenčík, 1990, Vertical seismic profile synthetics by dynamic ray tracing in laterally varying layered anisotropic structures: J. Geophys. Res., **95**, 11301–11315.

Golikov, P. and A. Stovas, 2010, New weak-contrast approximation for reflection coefficients in transversely isotropic media: Journal of Geophysics and Engineering, **7**, 343–350.

Ivanov, Y., and A. Stovas, 2017, Weak-anisotropy approximation for P-wave reflection coefficient at the boundary between two tilted transversely isotropic media: Geophysical Prospecting, **65**, 485–502.

Jin, S., and A. Stovas, 2020a. Reflection and transmission approximations for weak contrast orthorhombic media: Geophysics, **85**, C37–C59.

Jin, S., and A. Stovas, 2020b. Reflection and transmission approximations for monoclinic media with a horizontal symmetry plane: Geophysics, **85**, C13–C36.

Klimeš, L., 2003. Weak-contrast reflection–transmission coefficients in a generally anisotropic background: Geophysics, **68**, 2063–2072.

Neves, F. A., and M. V. de Hoop, 2000, Some remarks on nonlinear AVA inversion in anisotropic media: Geophysics, **65**, 158–166.

Pšenčík, I., and V. Farra, 2017, Reflection moveout approximations for P-waves in a moderately anisotropic homogeneous tilted transverse isotropy layer: Geophysics, **82**, C175–C185.

Pšenčík, I. and J. L. Martins, 2001, Properties of weak contrast PP reflection/transmission coefficients for weakly anisotropic media. Stud. geophys. geod., **45**, 176–199.

Rüger, A., 1997, P-wave reflection coefficients for transversely isotropic models with vertical and horizontal axis of symmetry: Geophysics, **62**, 713–722.

Thomsen, L., 1986, Weak elastic anisotropy: Geophysics, **51**, 1954–1966.

Thomsen,L., 1993, Weak anisotropic reflections, *in* Castagna, J.P., and Backus,M.M., Eds., Offset-dependent reflectivity - theory and practice of AVO Analysis, SEG, Investigations in Geophysics, **8**, 103–111.

Tsvankin, I., and V. Grechka, 2011, Seismology of Azimuthally Anisotropic Media and Seismic Fracture Characterization: SEG.

Ursin, B., and G. V. Haugen, 1996, Weak-contrast approximation of the elastic scattering matrix in anisotropic media: Pageoph, 148, 685–714.

Vavryčuk, V. and I. Pšenčík, 1998, PP wave reflection coefficients in weakly anisotropic media: Geophysics, **63**, 2129–2141.

Zillmer, M., D. Gajewski, and B. M. Kashtan, 1997, Reflection coefficients for weak anisotropic media: Geophysical Journal International, **129**, 389–398.